

# Hadronization and Charm-Hadron Ratios in Heavy-Ion Collisions

Min He<sup>1</sup> and Ralf Rapp<sup>2</sup>

<sup>1</sup>*Department of Applied Physics, Nanjing University of Science and Technology, Nanjing 210094, China and*

<sup>2</sup>*Cyclotron Institute and Department of Physics and Astronomy,  
Texas A&M University, College Station, Texas 77843-3366, U.S.A.*

(Dated: May 23, 2019)

Understanding the mechanisms of hadronization of the quark-gluon plasma (QGP) remains a challenging problem in the study of strong-interaction matter as produced in ultrarelativistic heavy-ion collisions (URHICs). The large mass of heavy quarks renders them excellent tracers of the color neutralization process of the QGP. Based on the resonance recombination model, we develop a 4-momentum conserving framework for the formation of heavy-flavor (HF) mesons and baryons that recovers the thermal and chemical equilibrium limits for their spectra and yields. Our framework explicitly accounts for space-momentum correlations of heavy quarks with the partons of the hydrodynamically expanding QGP that are difficult to control in instantaneous coalescence models. These correlations cause fast-moving heavy quarks to preferentially recombine with high-flow thermal quarks in the outer regions of the fireball, which we find to play a crucial role in explaining the  $\Lambda_c/D^0$  ratio as recently observed in URHICs. Another critical ingredient is the improved chemistry of our approach, in particular a large set of “missing” charm-baryon states which were previously shown to account for the large  $\Lambda_c^+/D^0$  ratio observed in proton-proton collisions at the LHC. When implemented into our HF hydro-Langevin-recombination framework for the strongly-coupled QGP, we find a good overall description of available HF data at RHIC and the LHC.

PACS numbers: 25.75.-q 25.75.Dw 25.75.Nq

*Introduction.*— Ultra-relativistic heavy-ion collisions (URHICs) at RHIC and the LHC have created a novel state of strong-interaction matter composed of deconfined quarks and gluons, known as Quark-Gluon Plasma (QGP) [1, 2]. The QGP behaves like a near-perfect fluid with small specific shear viscosity, as revealed by the collective-flow pattern of the final-state hadron spectra being consistent with relativistic hydrodynamic simulations [3–5]. A closely related discovery is the surprisingly large collective flow observed for heavy-flavor (HF) particles and quantified by a small diffusion coefficient,  $\mathcal{D}_s$  [6, 7], corroborating the strongly-coupled nature of the QGP. Another interesting finding is an enhancement of baryon-to-meson ratios ( $p/\pi$  and  $\Lambda/K$ ), relative to  $pp$  collisions, at intermediate transverse momenta,  $p_T \simeq 3\text{--}4\text{ GeV}$ , together with the so-called constituent-quark number scaling (CQNS) of the elliptic flow,  $v_2$ , of baryons and mesons. These observations have been attributed to quark coalescence processes as a hadronization mechanism of kinetic (non-thermalized) partons with thermal partons in the QGP [8–11]. The question arises as to whether the prominent phenomena described above could have a common origin.

The diffusion properties of low-momentum HF particles have long been recognized as an excellent gauge of their interaction strength with the medium, most notably through their elliptic flow acquired in non-central URHICs via a drag from the collectively expanding fireball, *c.f.* [7] for a recent review. The large mass of heavy quarks,  $m_Q \gg T_H$  (with  $T_H \simeq 160\text{ MeV}$  the typi-

cal hadronization temperature [12]), also provides a clean window on their hadronization processes. Thus, HF spectra simultaneously encompass the at first sight unrelated phenomena described above. An important role is also played by the chemistry of the produced HF hadrons [13–17], which has recently drawn a lot of attention through the observed enhancements in the  $D_s/D^0$  and  $\Lambda_c/D^0$  ratios at RHIC [18, 19] and the LHC [20, 21]. A reliable interpretation of these data requires a hadronization model that satisfies both kinetic and chemical equilibrium in the limit of thermal quark distributions as an input. This is also a pre-requisite for an ultimate precision extraction of the HF transport coefficients, reinforcing the intimate relation between heavy-quark (HQ) diffusion and hadronization. In the kinetic sector, this has been realized in the resonance recombination model (RRM) [22], where an explicit mapping from equilibrium quark spectra to equilibrium  $D$ -meson spectra in URHICs, including their elliptic flow, has been demonstrated on a hydrodynamic hypersurface [23]. At the same time, the RRM directly connects to the resonance correlations that develop near  $T_H$  in the heavy-light  $T$ -matrix interactions [24], which importantly figure in the HQ diffusion processes in the QGP.

In this work, we generalize RRM and its implementation in several critical aspects that will allow us to address the  $\Lambda_c/D^0$  “puzzle” in a comprehensive set-up for HF observables. First, we develop an extension to the three-body case necessary to treat hadronization into baryons, and verify the equilibrium mapping from 3-

quark into baryon spectra. Second, we implement RRM event-by-event (EbyE) for charm- ( $c$ -) quark distributions obtained from Langevin simulations, which maintains  $c$ -quark number conservation and satisfies the equilibrium limit of the charm-hadron *chemistry*. Our formalism explicitly accounts for space-momentum correlations (SMCs) of  $c$  quarks with those of the underlying hydro background. The treatments of both hadro-chemistry and quark SMCs have been challenging within instantaneous coalescence models (ICMs) [25]. Third, the equilibrium limit of the charm-hadron chemistry is improved by employing an enlarged set of “missing” charm-baryon states beyond the particle data group (PDG) listing, but motivated by lattice-QCD (lQCD) calculations and recent analysis of the large  $\Lambda_c^+/D^0$  ratio measured in  $pp$  collisions at the LHC [26].

*Baryons in RRM.*— Let us first recall the main features of the two-body RRM [22]. Starting from the Boltzmann equation, resonant quark-antiquark scattering into mesons, near equilibrium,  $q + \bar{q} \leftrightarrow M$ , can be utilized to equate gain and loss terms and arrive at a meson phase space distribution (PSD) of the form

$$f_M(\vec{x}, \vec{p}) = \frac{\gamma_M(p)}{\Gamma_M} \int \frac{d^3\vec{p}_1 d^3\vec{p}_2}{(2\pi)^3} f_q(\vec{x}, \vec{p}_1) f_{\bar{q}}(\vec{x}, \vec{p}_2) \times \sigma_M(s) v_{\text{rel}}(\vec{p}_1, \vec{p}_2) \delta^3(\vec{p} - \vec{p}_1 - \vec{p}_2), \quad (1)$$

where  $f_{\bar{q},q}$  are the anti-/quark PSDs,  $v_{\text{rel}}$  their relative velocity,  $\gamma_M(p) = E_M(p)/m_M$ , and  $\Gamma_M$  the meson width. The latter, together with the meson mass  $m_M$  and degeneracy factors, also figure in the resonant  $q + \bar{q} \rightarrow M$  cross section, usually taken of Breit-Wigner type.

The generalization to the three-body case is conducted in two steps. First, quark-1 and quark-2 recombine into a diquark resonance,  $q_1(\vec{p}_1) + q_2(\vec{p}_2) \rightarrow dq(\vec{p}_{12})$ , whose PSD is obtained in analogy to meson formation, by replacing  $M \rightarrow dq$ ,  $q \rightarrow q_1$  and  $\bar{q} \rightarrow q_2$  in Eq. (1). Second, the diquark recombines with quark-3 forming a baryon by reusing Eq. (1), to obtain

$$f_B(\vec{x}, \vec{p}) = \frac{\gamma_B}{\Gamma_B} \int \frac{d^3\vec{p}_1 d^3\vec{p}_2 d^3\vec{p}_3}{(2\pi)^6} \frac{\gamma_{dq}}{\Gamma_{dq}} f_1(\vec{x}, \vec{p}_1) f_2(\vec{x}, \vec{p}_2) \times f_3(\vec{x}, \vec{p}_3) \sigma_{dq}(s_{12}) v_{\text{rel}}^2 \sigma_B(s) v_{\text{rel}}^{dq3} \delta^3(\vec{p} - \vec{p}_1 - \vec{p}_2 - \vec{p}_3). \quad (2)$$

where  $s_{12} = (p_1 + p_2)^2$ ,  $s = (p_1 + p_2 + p_3)^2$ ,  $\sigma_B$ : resonance cross section for  $dq + q \rightarrow B$ . This expression depends on the underlying three-quark PSDs on an equal footing.

To check the equilibrium mapping of quark into hadron spectra, we calculate the PSDs for recombination of thermal  $c$  and light quarks ( $q$ ) into  $D^0$  and  $\Lambda_c^+$ , using  $f_{c,q}^{\text{eq}}(\vec{x}, \vec{p}) = g_{c,q} e^{-p \cdot u(x)/T_H}$  with a flow velocity  $u(x)$  on a hydrodynamic hypersurface at  $T_H = 170$  MeV for 0-20% Pb-Pb ( $\sqrt{s_{\text{NN}}}=5.02$  TeV) collisions [27] (with quark masses  $m_c=1.5$  GeV,  $m_q=0.3$  GeV and diquark

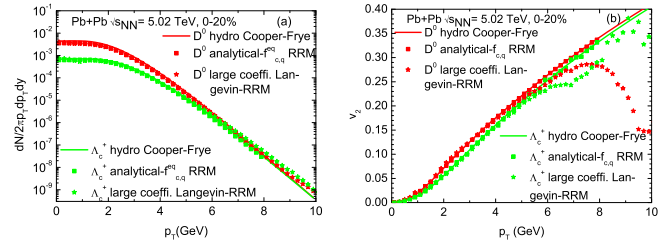


FIG. 1: (Color online) RRM mapping of thermal light- and  $c$ -quark distributions (boxes: thermal, stars: from Langevin simulations with large relaxation rate) into (a)  $p_T$ -spectra and (b)  $v_2$  of  $D^0$  and  $\Lambda_c^+$ , compared to direct  $D^0$  and  $\Lambda_c^+$  hydro results (lines).

mass  $m_{ud}=0.7$  GeV). The invariant hadron spectra,

$$\frac{dN_{M,B}}{p_T dp_T d\phi_p dy} = \int \frac{p \cdot d\sigma}{(2\pi)^3} f_{M,B}(\vec{x}, \vec{p}) \quad (3)$$

( $d\sigma_\mu$ : hypersurface element), displayed in Fig. 1, confirm that the RRM-generated hadron  $p_T$ -spectra agree with their direct calculation on the same hypersurface in chemical equilibrium, including their elliptic flow  $v_2$ , demonstrated here for the first time for baryons.

*Space-momentum correlations.*— The original derivation of CQNS for light-hadron elliptic flow within ICMs assumed spatially homogeneous (“global”) quark distributions in the fireball,  $v_2^q(\vec{x}, \vec{p}) = v_2^q(\vec{p})$  [8, 9]. This is incompatible with hydrodynamic flow fields and rendered CQNS to be very fragile upon including realistic SMCs [11]. The application of RRM in the mesonic sector [28] could resolve this problem, but no explicit signature of SMCs from recombination processes was identified. Here, we propose that the recent results for the  $\Lambda_c/D^0$  ratio are such a signature, utilizing our previously developed hydro-Langevin approach [23], a strong-coupling framework for both bulk evolution and transport coefficients (obtained from microscopic HQ interactions from a thermodynamic  $T$ -matrix [24]), as developed and applied previously to HF observables at RHIC [15] and the LHC [29]. The underlying SMCs are illustrated in Fig. 2 for  $c$ -quark distributions in the transverse plane in different  $p_T$  bins at hadronization. Clearly, low- $p_T$  (0-1 GeV) and higher- $p_T$  (3-4 GeV)  $c$  quarks preferentially populate the inner and outer regions of the fireball, respectively. The spatial density,  $dN/d^3x$ , of Cooper-Frye generated thermal light-quark spectra (at midrapidity) from the underlying hydro evolution on the same hypersurface shows a similar behavior. As recombination occurs between partons close to each other in both  $\vec{x}$  and  $\vec{p}$  space, the SMCs (not included in previous studies [16, 17] using ICMs) are expected to play an important role in the recombination of  $c$  and light quarks into charm hadrons, especially at intermediate  $p_T$  where the signals of the baryon enhancement are prominent.

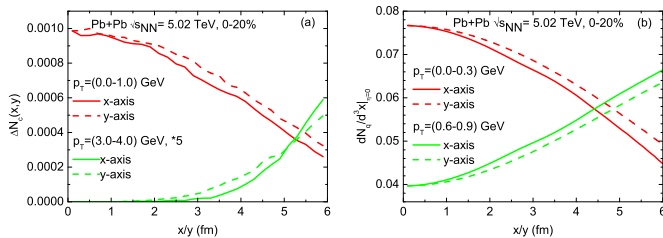


FIG. 2: (Color online) Spatial distributions of (a)  $c$ -quarks from Langevin simulations and (b) light quarks from the underlying hydro medium in the transverse fireball plane in different  $p_T$  bins.

*EbyE Langevin-RRM.*— To achieve the inclusion of SMCs together with exact  $c$ -quark number conservation, we implement the RRM EbyE in the fluid rest frame, seamlessly following the Langevin simulation of  $c$ -quark diffusion. Toward this end, we first determine the  $c$ -quark recombination probability self-consistently from the RRM formalism.

Using the PSDs in the fluid restframe (starred variables) of a homogeneous hydro cell for thermal light-quarks at temperature  $T_H$ ,  $f_{\bar{q}}(\vec{x}^*, \vec{p}_1^*) = g_q e^{-E(\vec{p}_1^*)/T_H}$ , and a single  $c$ -quark,  $f_c(\vec{x}^*, \vec{p}_2^*) = (2\pi)^3 \delta^3(\vec{p}_2^* - \vec{p}_c^*)/V^*$ , we apply Eq. (1) to obtain

$$N_M(p_c^*) = \int \frac{d^3\vec{p}_1^*}{(2\pi)^3} g_q e^{-E(\vec{p}_1^*)/T_H} \frac{\gamma_M}{\Gamma_M} \sigma(s) v_{\text{rel}}, \quad (4)$$

which characterizes the recombination probability to form charm meson  $M$  from a  $c$ -quark of momentum  $\vec{p}_c^*$ . Similarly, using two light-quark thermal distributions in Eq. (2), the counterpart for charm baryons reads

$$N_B(p_c^*) = \frac{\gamma_B}{\Gamma_B} \int \frac{d^3\vec{p}_1^* d^3\vec{p}_2^*}{(2\pi)^6} g_1 e^{-E(\vec{p}_1^*)/T_H} g_2 e^{-E(\vec{p}_2^*)/T_H} \times \frac{\gamma_{dq}}{\Gamma_{dq}} \sigma(s_{12}) v_{\text{rel}}^{12} \sigma(s_{d3}) v_{\text{rel}}^{d3}. \quad (5)$$

The  $N_{M,B}(p_c^*)$  are evaluated for charm mesons and baryons (including strangeness with  $m_s=0.4$  GeV and  $m_{us}=0.80$  GeV) with resonance widths  $\Gamma_M \simeq 0.1$  GeV,  $\Gamma_{dq} \simeq 0.2$  GeV and  $\Gamma_B \simeq 0.3$  GeV, compatible with the values from the thermodynamic  $T$ -matrix [24]. We have checked that our final results are robust against variation of the resonance widths by  $\sim 0.1$  GeV.

To evaluate recombination of individual  $c$ -quark Langevin events on their respective hydro hypersurface element,  $d\sigma_H$ , at  $T_H$ , we prepare a sampling of the static thermal light-quark PSD  $f_q(\vec{x}^*, \vec{p}_1^*) \sim \sum_n \delta^3(\vec{p}_1^* - \vec{p}_{1n}^*)$ . Using Lorentz invariance of the meson PSD,  $f_M(\vec{x}, \vec{p}) = f_M(\vec{x}^*, \vec{p}^*)$  ( $\vec{x}$  and  $\vec{p}$  denote labframe variables), and of  $E_M(\vec{p}^*) \delta^3(\vec{p}^* - \vec{p}_{1n}^* - \vec{p}_c^*) = E_M(\vec{p}) \delta^3(\vec{p} - \vec{p}_{1n} - \vec{p}_c)$ , substitution of  $f_M(\vec{x}, \vec{p})$  into Eq. (3) results in

$$\frac{dN_M}{d\eta} \Big|_{\eta=0} \equiv \sum_n \Delta N_M[n] = \sum_n \frac{p \cdot d\sigma_H}{m_M \Gamma_M} \sigma(s) v_{\text{rel}}, \quad (6)$$

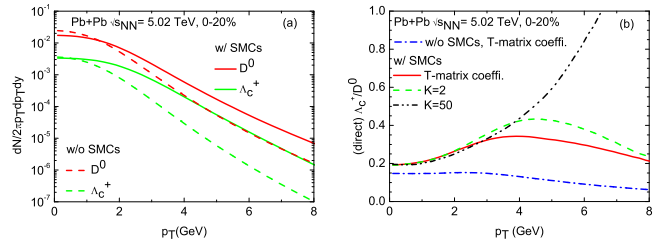


FIG. 3: (Color online) (a): Direct  $D^0$  and  $\Lambda_c^+$  spectra from hydro-Langevin-RRM simulations with baseline  $T$ -matrix  $c$ -quark thermalization rate, in comparison with the counterparts without SMCs. (b): The pertinent  $\Lambda_c^+/D^0$  ratio with (red line) and without (dash-dotted line) SMCs, and when using a  $K$ -factor of 2 (dashed line) and 50 (dash-double dotted line) in the baseline  $T$ -matrix rate including SMCs.

where  $\vec{p} = \vec{p}_{1n} + \vec{p}_c$  is the labframe meson momentum. The  $\Delta N_M[n]$ 's form a momentum distribution, whose sum is then renormalized to the *absolute* recombination probability  $N_M(p_c^*)$ . The renormalized  $\Delta N_M[n]$ 's are binned into  $(p_T, \phi_p)$  histograms to yield the invariant meson spectra,  $dN_M/p_T dp_T d\phi_p d\eta$ . An analogous procedure is conducted for charm baryons by sampling two static thermal-light quark PSDs to obtain the invariant baryon spectrum,  $dN_B/p_T dp_T d\phi_p d\eta$ .

*Direct  $\Lambda_c^+/D^0$  ratio from RRM.*— We now deploy the EbyE Langevin-RRM simulation with  $T$ -matrix transport coefficients in the QGP [24], first focusing on the *direct* production of  $\Lambda_c$  and  $D^0$  hadrons (*i.e.*, without the inclusion of feeddown from excited states). The initial  $c$ -quark spectra are taken from the FONLL package [30] as used in our recent description of ALICE HF data in  $\sqrt{s}=5.02$  TeV  $pp$  collisions [26].

The resulting RRM-generated spectra of  $D^0$  and  $\Lambda_c^+$  and their ratio right after hadronization at  $T_H=170$  MeV are shown in Fig. 3, with and without the inclusion of SMCs. The SMCs cause the  $D^0$  and  $\Lambda_c^+$  spectra to be significantly harder, and the pertinent ratio  $\Lambda_c^+/D^0$  ratio is much enhanced at intermediate  $p_T=3-6$  GeV, relative to their counterparts without SMCs (where RRM is carried out in momentum space only). The key role is played by the relatively fast  $c$  quarks moving to the outer parts of the fireball where, upon including SMCs, a higher density of significantly harder light-quark spectra is available for recombination, an effect that enters squared for production of  $\Lambda_c$  baryons. Consequently, their RRM yield toward larger labframe  $p_T$  is appreciably enhanced relative to  $D^0$  mesons.

We have numerically verified that in the limit of large  $c$ -quark thermalization rates, the *absolute*  $p_T$  spectra and  $v_2$  of  $D^0$  and  $\Lambda_c^+$  from the EbyE Langevin-RRM simulation agree well with the direct hydro calculation (recall Fig. 1), *i.e.*, the “equilibrium mapping” is maintained in the presence of SMCs. Also illustrated in Fig. 3 is that

using a  $K$ -factor of 2 in the HQ thermalization rate only yields a modest enhancement of the  $\Lambda_c/D^0$  ratio over the baseline calculation, much less than the SMC effect.

*Charm Conservation.*— As is well known from the light-hadron sector, feeddown from excited states is an essential component in the description of soft-hadron production in both elementary and heavy-ion collisions. This is also expected for charm-hadron production, with the difference that the total number of produced  $c\bar{c}$  pairs is imprinted into the system from hard production and essentially conserved thereafter. To enforce this in our framework, we assume that the total recombination probability for a  $p^*=0$   $c$ -quark, summed over all charm hadrons, is unity (*i.e.*, all  $N_{M,B}(p_c^*)$  are scaled by a *common* factor), as there is neither excess energy nor momentum available for fragmentation. The RRM with its built-in chemical equilibrium limit then predicts the relative abundance and  $p_T$  dependence of all charm-hadron species. We recall that a critical ingredient here is the largely augmented charm-baryon spectrum (beyond the PDG listings), which, via feeddown, leads to a factor  $\sim 2$  enhancement of the  $\Lambda_c/D^0$  ratio in  $pp$  collisions, in fair agreement with ALICE midrapidity data. With increasing  $p_T$ ,  $c$  quarks that are not hadronized via RRM will be converted into charm hadrons using standard fragmentation functions with a chemistry determined by high- $p_T$  production in  $pp$  collisions [26]. The last ingredient needed to obtain the total norm of the charm-hadron spectra (equivalent to a charm-quark fugacity at  $T_H$ ) is the total charm cross section (which does not affect any ratio of charm hadrons). With a value of  $d\sigma_{c\bar{c}}/dy=1.0$  mb taken from midrapidity ALICE 5.02 TeV  $pp$  data [26], a binary nucleon-nucleon collision number of  $N_{\text{coll}}\simeq 1370$  and a  $\sim 20\%$  shadowing [31] for 0-20%  $\sqrt{s_{\text{NN}}}=5.02$  TeV Pb-Pb collisions, we obtain  $dN_c/dy\simeq 15.4$ .

*Charm-Hadron Spectra and Ratios.*— To enable quantitative comparisons of our EbyE-Langevin-RRM simulations to experimental data for charm-hadron nuclear modification factors and  $v_2$ , we include two further ingredients. First, we continue the Langevin simulations for all hadrons through the hadronic phase, starting from their PSDs right after hadronization (*i.e.*, after RRM + fragmentation) until kinetic freezeout of the hydrodynamic evolution at  $T_{\text{kin}}=110$  MeV (as obtained from fits to bulk-hadron spectra and  $v_2$ ). For  $D$ -mesons we employ previously calculated thermalization rates [32]; for charm baryons we scale the  $D$ -meson rates with a factor of  $E_D(p^*)/E_{\Lambda_c}(p^*)$  to account for their higher masses. The uncertainty due to hadronic diffusion will be illustrated in our plots below. Second, since our focus here is on hadronization mechanisms, and our approach currently does not include radiative energy loss, we allow ourselves a temperature- and momentum-independent  $K$ -factor of 1.6 in the QGP diffusion rate, chosen to improve the overall description of the LHC and RHIC data.

The spectra of all excited states are used to perform

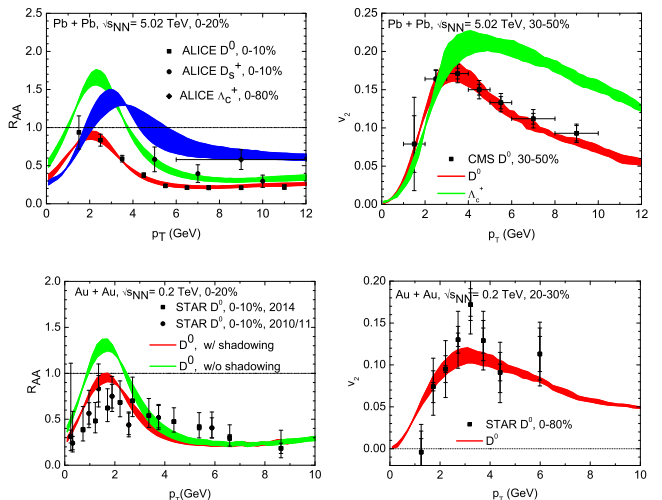


FIG. 4: (Color online)  $R_{AA}$  (left panels) and  $v_2$  (right panels) of  $D^0$ ,  $D_s^+$  and  $\Lambda_c^+$  in Pb-Pb(5.02 TeV) (upper panels) and Au-Au(0.2 TeV) collisions (lower panels), compared to data [20, 21, 33, 34]. The bands encompass the results with and without hadronic diffusion.

decay simulations (following our recent calculations for the  $pp$  baseline [26]) to obtain the final spectra of the ground-state  $D^0$ ,  $D^+$ ,  $D_s^+$  and  $\Lambda_c^+$ , which are then converted into nuclear modification factors

$$R_{AA}(p_T) = \frac{dN_{AA}/dp_T}{N_{\text{coll}}dN_{pp}/dp_T}, \quad (7)$$

elliptic flows  $v_2(p_T)$  and ratios  $D_s^+/D^0$  and  $\Lambda_c^+/D^0$ . We compare our results to a selection of RHIC and LHC data in 0.2 TeV Au-Au and 5.02 TeV Pb-Pb data, respectively, in Figs. 4 and 5). The hierarchy of the suppression observed in the  $R_{AA}$  for  $D^0$ ,  $D_s^+$  and  $\Lambda_c^+$  at the LHC are well reproduced, and consequently their ratios. The key reason for this, relative to our earlier calculations, is the larger reach in  $p_T$  of the recombination contribution, critically enabled by the SMCs of fast-moving  $c$ -quarks with the high-flow partons in the outer regions of the fireball. Another remarkable consequence of the SMCs in the RRM is that the  $D$ -meson  $v_2$  data are much better described out to higher  $p_T$  than our previous results. For the description of the  $\Lambda_c/D^0$  enhancement, another essential ingredient is the larger equilibrium limit as put forward in our recent work [26]. At RHIC, our results for the  $D^0$ - $R_{AA}$ , without nuclear shadowing, overestimate the low- $p_T$  STAR data [33] significantly. A scenario with  $\sim 20\%$  shadowing works better, although current nuclear PDFs do not favor such a scenario. The RHIC results for the  $D^0$   $v_2$  as well as the  $\Lambda_c/D^0$  and  $D_s^+/D^0$  ratios are virtually independent of shadowing and reasonably agree with the pertinent STAR data.

*Summary.*— In an attempt to understand recent measurements of various charm-hadron data in URHICs, we have advanced the description of their hadronization in

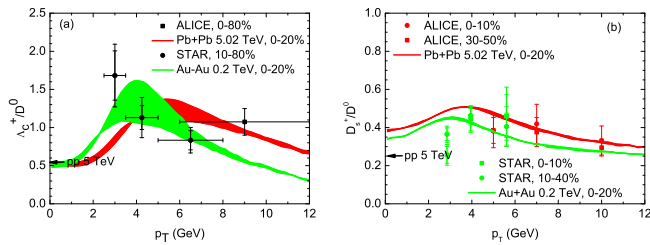


FIG. 5: (Color online) (a):  $\Lambda_c^+/D^0$  and (b):  $D_s^+/D^0$  ratios compared to data [18–21] in Pb-Pb(5.02 TeV) collisions. The bands encompass the uncertainty due to hadronic diffusion. The horizontal arrows denote the pertinent  $pp$  values [26].

three critical aspects. First, we extended the resonance recombination model to baryons, with an explicit kinetic-equilibrium mapping from quarks to hadrons, which is essential for theoretically controlled calculations. Second, we implemented space-momentum correlations between  $c$ -quarks and the hydro medium. Third, we incorporated an improved charm-hadrochemistry with a much extended charm-baryon spectrum (enhancing the feeddown to  $\Lambda_c$ ), as previously tested in  $pp$  collisions. We have deployed these developments within our non-perturbative hydro-Langevin-RRM framework, thereby allowing for a moderate  $K$  factor in the QGP diffusion coefficients to simulate hitherto missing contributions (such as radiative interactions). We have found that all three developments play a key role in a quantitative description of the LHC and RHIC data: the SMCs of fast-moving  $c$ -quarks with high-flow partons in the fireball decisively extend the  $p_T$  reach of recombination processes which, together with the augmented chemistry, can explain the  $\Lambda_c$  and  $D_s$  enhancements observed at intermediate  $p_T$ . In addition, the SMC's significantly increase the charm-hadron  $v_2$  in this region, in good agreement with RHIC and LHC  $D$ -meson data. Future developments will now focus on improving the microscopic HQ interactions in the QGP, with lQCD vetted potentials and radiative processes, as well as using a more refined hydrodynamic evolution. Our approach can be straightforwardly tested in the bottom sector and may be useful for revisiting coalescence models in the light-quark sector. It is also expected to improve the precision in extracting the HF diffusion coefficient in QCD matter.

*Acknowledgments.* – This work was supported by NSFC grant 11675079 and the U.S. NSF under grant PHY-1614484.

- 
- [1] Y. Akiba *et al.*, arXiv:1502.02730 [nucl-ex].  
 [2] E. Shuryak, Rev. Mod. Phys. **89**, 035001 (2017).  
 [3] U. Heinz and R. Snellings, Ann. Rev. Nucl. Part. Sci. **63**, 123 (2013);

- [4] C. Gale, S. Jeon and B. Schenke, Int. J. Mod. Phys. A **28**, 1340011 (2013).  
 [5] H. Niemi, K. J. Eskola and R. Paatelainen, Phys. Rev. C **93**, no. 2, 024907 (2016).  
 [6] R. Rapp *et al.*, Nucl. Phys. A **979**, 21 (2018).  
 [7] X. Dong, Y. J. Lee and R. Rapp, arXiv:1903.07709 [nucl-ex].  
 [8] V. Greco, C. M. Ko and P. Levai, Phys. Rev. Lett. **90**, 202302 (2003); Phys. Rev. C **68**, 034904 (2003).  
 [9] R. J. Fries, B. Muller, C. Nonaka and S. A. Bass, Phys. Rev. Lett. **90**, 202303 (2003); Phys. Rev. C **68**, 044902 (2003).  
 [10] R. C. Hwa and C. B. Yang, Phys. Rev. C **67**, 064902 (2003).  
 [11] D. Molnar and S. A. Voloshin, Phys. Rev. Lett. **91**, 092301 (2003).  
 [12] A. Andronic, P. Braun-Munzinger, K. Redlich and J. Stachel, Nature **561**, no. 7723, 321 (2018).  
 [13] A. Andronic, P. Braun-Munzinger, K. Redlich and J. Stachel, Phys. Lett. B **659**, 149 (2008).  
 [14] I. Kuznetsova and J. Rafelski, Eur. Phys. J. C **51**, 113 (2007).  
 [15] M. He, R. J. Fries and R. Rapp, Phys. Rev. Lett. **110**, no. 11, 112301 (2013).  
 [16] Y. Oh, C. M. Ko, S. H. Lee and S. Yasui, Phys. Rev. C **79**, 044905 (2009).  
 [17] S. Plumari, *et al.*, Eur. Phys. J. C **78**, no. 4, 348 (2018).  
 [18] L. Zhou [STAR Collaboration], Nucl. Phys. A **967**, 620 (2017).  
 [19] S. Radhakrishnan [STAR Collaboration], Nucl. Phys. A **982**, 659 (2019).  
 [20] S. Acharya *et al.* [ALICE Collaboration], JHEP **1810**, 174 (2018).  
 [21] S. Acharya *et al.* [ALICE Collaboration], Phys. Lett. B **793**, 212 (2019).  
 [22] L. Ravagli and R. Rapp, Phys. Lett. B **655**, 126 (2007).  
 [23] M. He, R. J. Fries and R. Rapp, Phys. Rev. C **86**, 014903 (2012).  
 [24] F. Riek and R. Rapp, Phys. Rev. C **82**, 035201 (2010); K. Huggins and R. Rapp, Nucl. Phys. A **896**, 24 (2012).  
 [25] R. J. Fries, V. Greco and P. Sorensen, Ann. Rev. Nucl. Part. Sci. **58**, 177 (2008).  
 [26] M. He and R. Rapp, arXiv:1902.08889 [nucl-th].  
 [27] M. He, R. J. Fries and R. Rapp, Nucl. Part. Phys. Proc. **289-290**, 265 (2017).  
 [28] L. Ravagli, H. van Hees and R. Rapp, Phys. Rev. C **79**, 064902 (2009).  
 [29] M. He, R. J. Fries and R. Rapp, Phys. Lett. B **735**, 445 (2014).  
 [30] M. Cacciari, M. Greco and P. Nason, JHEP **9805**, 007 (1998); JHEP **0103**, 006 (2001).  
 [31] K. J. Eskola, H. Paukkunen and C. A. Salgado, JHEP **0904**, 065 (2009).  
 [32] M. He, R. J. Fries and R. Rapp, Phys. Lett. B **701**, 445 (2011).  
 [33] L. Adamczyk *et al.* [STAR Collaboration], Phys. Rev. Lett. **113**, no. 14, 142301 (2014), and Erratum: [Phys. Rev. Lett. **121**, no. 22, 229901 (2018)]; J. Adam *et al.* [STAR Collaboration], Phys. Rev. C **99**, no. 3, 034908 (2019).  
 [34] L. Adamczyk *et al.* [STAR Collaboration], Phys. Rev. Lett. **118**, no. 21, 212301 (2017).